necrosis factor-α conjugated with polyvinylpyrrolidone on solid tumors in mice. *Cancer Res.*, **60**: 6416-6420, 2000.
7) Kaneda, Y. et al.: Antitumor activity of tumor necrosis factor-α conjugated with diviny ether and maleic anhydride copolymer on solid tumors in mice. *Cancer Res.*, **58**(2): 290-295, 1998.
8) Tsutsumi, Y. et al.: PEGylation of interleukin-6 effectively increases its thrombopoietic potency. *Thromb. Haemost.*, **77**: 168-173, 1997.
9) Tsutsumi, Y. et al.: Molecular design of hybrid tumour necrosis factor alpha with polyethylene glycol increases its anti-tumour potency. *Br. J. Cancer*, **71**: 963-968, 1995.
10) Tsutsumi, Y. et al.: Molecular design of hybrid tumour necrosis factor-α II: The molecular size of polyethylene glycol-modified tumour necrosis factor-α affect its anti-tumour potency. *Br. J. Cancer*, **74**: 1090-1095, 1996.
11) Tsutsumi, Y. et al.: Molecular design of hybrid tumor necrosis factor-α III: Polyethylene glycol-modified tumor necrosis factor-α has markedly enhanced anti-tumor potency due to longer plasma half-life and higher tumor-accumulation. *J. Pharmacol. Exp. Ther.*, **278**: 1006-1011, 1996.
12) Yamagishi, J. et al.: Mutational analysis of structure-activity relationships in human tumor necrosis factor-α. *Protein Eng.*, **3**: 713-719, 1990.
13) Van Ostade, X. et al.: Localization of the active site of human tumour necrosis factor (hTNF) by mutational analysis. *Embo J.*, **10**: 827-836, 1991.
14) Loetscher, H. et al.: Human tumor necrosis factor alpha (TNFα) mutants with exclusive specificity for the 55 kDa or 75 kDa TNF receptors. *J. Biol. Chem.*, **268**: 26350-26357, 1993.
15) Jones, E. Y. et al.: Structure of tumour necrosis factor. *Nature*, **338**: 225-228, 1989.
16) Jones, C. A.: Serum creatinine levels in the US population: third National Health and Nutrition Examination Survey. *Am. J. Kidney Dis.*, **32**: 992-999, 1998.
17) Progress and Priorities: Renal disease research plan. Report of the strategic planning conferences-Renal research properties-sponsored by National Institute of Diabetes, and Digestive and Kidney Disease, Council of American Kidney Socities (December 5-6, 1998 and February 4-5, 1999). (http://www.niddk.nih.gov/federal/planning.htm#g)

薬 剤 学, 64 (3), 159–163 (2004)

≪若手研究者紹介≫

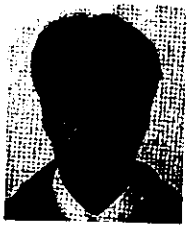

蛋白療法の最適化に叶うDDSの開発を目指して

堤　　康 央　Yasuo Tsutsumi
大阪大学薬学研究科薬剤学分野

1. は じ め に

若手研究者紹介コラムへの執筆機会を賜り，そのタイトルを思い巡らせ，最終的に上記とさせて頂いた．筆者は，学部学生として大阪大学薬学部薬剤学講座に配属してからの14年間，一貫してこのタイトルに取り組んできた．この間，国立循環器病センター研究所や米国の国立衛生研究所（NIH）への留学などにより，多くの先生方から最新の医用高分子化学，遺伝子工学，蛋白質工学をご教授賜り，研究の質的グレード・アップを図ってきたものの，その研究対象は遺伝子そのものではなく，常にその翻訳産物である蛋白質にあった．今改めて周りを見渡すと，蛋白質の医薬品化を目指したDDS研究，特にPEGylationに代表される蛋白質の高分子バイオコンジュゲーションにしがみついているのは筆者ぐらいなもので，恩師　真弓忠範先生からの叱咤激励と情熱，愛情が無ければ，途中で挫折していたかもしれない．その真弓忠範先生が，この2004年3月31日付けで大阪大学をご停年退官される．本稿では，これまでの想いを込めて，上記タイトルに関して，我々がこれまで歩んできた道のりの一端を，紙面の許す限り，紹介させて頂きたい．

筆者紹介：1991年3月大阪大学薬学部薬学科卒業，同年4月国立循環器病センター研究所生体工学部研究員（松田武久先生），1993年3月大阪大学大学院薬学研究科応用薬学専攻修士課程修了，1994年8月大阪大学大学院薬学研究科応用薬学専攻博士課程中退後，直ちに大阪大学薬学部助手，1997年8月薬学博士（大阪大学），現在に至る．この間，1999年4月～2001年1月米国National Cancer Institute (NCI) /National Institutes of Health (NIH) 博士研究員（Laboratory of Molecular Biology【Dr. Ira PASTAN】）に留学．平成9年度日本薬学会近畿支部奨励賞，平成16年度日本薬学会奨励賞，平成16年度日本薬剤学会奨励賞などを受賞．

2. プロテオーム創薬と21世紀型蛋白療法

ヒトゲノム解読が完了し，ポストゲノム研究は蛋白質の時空間的，質的，量的な機能発現様式と立体構造との連関を包括的に解明しようとするプロテオミクスや構造ゲノミクスへと集約されつつある．これは，ゲノムが単なる情報（遺伝型）に過ぎず，そのままでは何ら機能を発揮し得ないこと，転写したRNAが機能する極一部の例外を除き，このゲノム情報に基づき，多様な蛋白質群（プロテオーム；表現型）が翻訳され，その機能を発揮することで初めて生命現象が営めるようになることを考えると当然のことと言えよう．この研究の流れは，癌や種々感染症，自己免疫疾患などに対する抗体療法やサイトカイン療法といった21世紀医療が台頭してきたことも相俟って，疾病治療に有効な蛋白質を探索・創製しようとするプロテオーム創薬と，これらを適用した新規蛋白療法への期待を加速度的に高めている．

しかし過去の多くの事例が示しているように，蛋白質は一般に，体内安定性に極めて乏しいため，臨床応用の際には大量頻回投与を余儀なくされ，往々にして重篤な副作用を招いてしまう．なかでもサイトカインなどは，多彩な細胞上の複数種類のレセプターを介して，多様な *in vivo* 生理活性を示すため，目的とする治療作用のみならず副作用の原因となる他の作用までをも同時に発揮してしまう．そのため周知のように，医薬品化された蛋白質は極一部にすぎないのが現状である．従ってプロテオーム創薬や

21世紀型蛋白療法を推進するためには，このような蛋白質固有の問題点を克服できるDDSの確立が依然として必須となっている．本観点から我々は，(1) レセプター親和性・特異性などが高く，医薬価値に優れた機能性人工蛋白質を迅速創出できるネオ・ダーウィニズム的分子進化戦略（プロテオーム創薬システム）の構築[1]，(2) 蛋白質の生体内安定性を向上させ，かつ目的治療作用の選択的発現能を付与できる部位特異的高分子バイオコンジュゲーション法の確立[1~4]，(3)DDS機能（標的指向能・薬物徐放化能など）を有した高機能化修飾高分子の設計[5]など，上記三者を融合させた「蛋白療法の最適化に叶うDDSの確立」に関する研究を進めている．

3. プロテオーム創薬システム

蛋白療法の最適化に向け，従来から産官学の多くのバイオ研究機関が，特定レセプターへの親和性や選択性に優れた機能性人工蛋白質などを創製するため，Kunkel法といった点突然変異法を用いた構造変異蛋白質（アミノ酸置換体）の作製を精力的に試みている．しかし点突然変異法では，まず構造変異蛋白質の立体構造や機能をシミュレーションし，トライ・アンド・エラーで生理活性蛋白質の構成アミノ酸を一つずつ別の特定アミノ酸に改変することにより，個々の構造変異蛋白質を作製せねばならない．そのうえで目的とする機能性人工蛋白質を探索・同定するため，作製した構造変異蛋白質の諸機能を個別に評価する必要がある．そのため従来法では，時間ばかりが消費され，かつ作製し得る構造変異構造変異蛋白質の多様性（種類）にも限界があるなど，期待通りの成果は得られていない．そのため，より迅速かつ効率よく目的作用を有する機能性人工蛋白質を創製できるテクノロジーの開発が望まれている．

この点我々は最近，ファージ表面提示法を独自に改良することにより，蛋白質中の多数のアミノ酸を各々20種類のアミノ酸へ一挙に置換することで，10^8種類以上もの多様性を有した構造変異蛋白質をCombinatorial Biosynthesisし，この中からレセプター親和性・特異性などの高い「医薬価値に優れた機能性人工蛋白質」を迅速かつ効率良く同定できる基盤テクノロジー（プロテオーム創薬システム）を確立した．例えばアラニン・スキャンといった従来の点突然変異法を用いた構造—活性相関研究により，腫瘍壊死因子（TNF-α）のLys 11やLys 65, Lys 90はその立体構造（三量体）形成やレセプター結合に必須の役割を担っているものと考えられていた．これはTNF-αに限らず，一般にリジン残基は多くの場合，生理活性蛋白質の高次構造形成やリガンド—レセプター結合などに必須の役割を担っているため，他のアミノ酸への置換は致命的な活性低下を招いてしまうことが，従来までの点突然変異解析によって常識となっていた．事実これまで，活性を完全に保持させたまま，蛋白質中のリジン残基全てを欠損させ得た例（機能性リジン欠損体）は皆無であった．しかし我々はこの概念を覆す知見，即ちTNF-α中の全6個のリジン残基を一挙に他のアミノ酸へ置換しても，wild型TNF-α（wTNF-α）と同等から10倍以上ものレセプター親和性や生物活性を有する機能性リジン欠損TNF-αを創製することに初めて成功した．このwTNF-αと同等以上の生物活性を有する種々の機能性リジン欠損TNF-αは，BIAcoreを用いたTNFレセプター1やTNFレセプター2への結合性評価により，wTNF-αと同等以上のレセプター親和性を有していること，ゲル濾過解析などから三量体を形成していることも確認している．またこれらの機能性リジン欠損TNF-αの体内挙動を評価したところ，wTNF-αよりも血中滞留性に優れていることを認めた．この血中滞留性の向上は，カチオン性のリジン残基を他のアミノ酸へ置換したことによるLowering pI効果に起因したものと考えらる．さらにこれらの機能性リジン欠損TNF-αの*in vivo*における抗腫瘍効果は，Lowering pI効果により，wTNF-αと比較して数倍から10倍にまで向上しているうえ，その毒性は顕著に低下しており，その治療域はwTNF-αの十数倍以上にも向上していることが明らかとなった．これらの知見は，TNF-α分子中の全6個のリジン残基を他のアミノ酸へ一挙かつ網羅的に置換した20^6（6,400万）種類もの構造変異TNF-α（TNF-αのアミノ酸置換体）を表面提示したファージライブラリを作製したうえで，TNFレセプター1や抗TNF中和抗体に対するアフィニティー・バイオパンニングを行い，選択・濃縮された構造変異TNF-α群の諸機能を高速解析することによって得られたものである．即ち以上の事実は，ファージ表面提示法を駆使した基盤テクノ

ロジーを適用することで，今まで全く創造し得なかった医薬価値に優れた機能性人工蛋白質を新たに産み出し得ることを強く示しており，我々が確立した「プロテオーム創薬システム」は，他を圧倒する“プロテオーム創薬のための競争力(DDS基盤テクノロジー)”を提供するだけでなく，従来までの点突然変異法（アラニン・スキャン）で得られた知見では想像もでき得なかった“蛋白改変の概念”や“蛋白質の構造—活性相関概念”をも新たに提唱するものと期待している．

4. プロテオーム創薬のための バイオインフォマティクス

プロテオーム創薬は，プロテオミクスおよび構造ゲノミクスの進展と，これらの知見を統括したバイオインフォマティクスが駆動力となり，近い将来，上記の「プロテオーム創薬システム」との融合により加速度的に推進されるものと期待される．即ちこのようなプロテオーム創薬を指向したバイオインフォマティクスの進展は，蛋白質のアミノ酸配列（一次構造）と立体構造（三次構造），機能との連関を理解可能とするため，近未来的には蛋白質をコードした塩基配列や蛋白質のアミノ酸配列さえ判明すれば，その立体構造と機能が予測できることになる．これは逆に目的とする機能や立体構造を有した機能性蛋白質の新規デザインを可能とするだけでなく，蛋白質の立体構造やその機能を模倣した有機化合物の合理的設計をも可能にするものと期待される．このようなバイオインフォマティクスをシステムアップするためには，未知蛋白質の機能解明や立体構造解析に加え，種々の蛋白質について膨大な多様性を有する構造変異体を網羅的に作製し，レセプター・リガンド結合の様式，生物活性等をも含めた機能情報を集積し，立体構造との連関を追求しなけれならない．この点我々が開発した「プロテオーム創薬システム」は，視点を変えれば僅か1週間で10^8種類以上もの多様性を有する構造変異蛋白質のライブラリを作製し，その機能情報を高速集積できる基盤技術と言える．本観点から現在，機能性人工TNF-αを含む様々な構造変異蛋白質の機能評価と共に，そのX線結晶構造解析を進めており，近未来的なバイオインフォマティクスへの研究展開を予定している．

一方で最近，Gene shuffling や人工遺伝暗号システムなどを用いた機能性人工蛋白質の創出に注目が集まっている．これら興味深いアプローチは天然に存在しない新たなアミノ酸配列を有した蛋白質を人工的に作製しようとするものであるが，残念ながら臨床応用可能な非天然型生理活性蛋白質の創製には至っていない．当然のことながら，上述した我々の基盤テクノロジーはこれら非天然型生理活性蛋白質の探索や創製，安定化や高機能化にも適用可能であり，現在 Gene shuffling 法とファージ表面提示法を融合した新たな機能性人工蛋白質の創製システムの構築を進めている．

5. 部位特異的高分子バイオコンジュゲーション法

前述した(2)および(3)について我々は，主として酵素蛋白質への適用に限定されていたバイオコンジュゲーション法を，生理活性蛋白質一般に適用するためのグレードアップを図ってきた．その結果，1．蛋白質の作用機構を考慮し最適の修飾高分子を選択し，2．比活性—修飾率—分子サイズ等の相関をもとに最適条件を見出すことにより，①蛋白質の生体内安定性を飛躍的に向上させ得ること，②多様な *in vivo* 作用の中から，目的治療作用のみを数百倍にも高め得ることを明らかにしている．この②の生理活性蛋白質への作用の選択性付与は，投与量の削減や副作用発現組織への移行性低下に因ることを明らかにし，Interleukin-6 や TNF-α のバイオコンジュゲーションの場合，副作用を増幅することなく目的とする血小板産生促進効果や抗腫瘍効果が各々500倍および100倍にも選択増強されることを認めている．このようにバイオコンジュゲーションは蛋白質の医薬品開発において，最適 DDS 技術の地位を確立しつつあるが，その成功例は極めて少ない．この最大の原因は，水溶性高分子を蛋白質に結合させる際に，水溶性高分子がリジンεアミノ基やN末端αアミノ基へランダムに結合してしまうことにある．そのため，生理活性蛋白質の活性発現部位への結合は致命的な比活性低下をきたし，結合分子数・部位の違いはバイオコンジュゲート体の分子的・機能的不均一性をもたらす結果となる．我々はこれらの問題を解決するため，前述した①を応用して，生理活性蛋白質の活性を完全に保持したリジン欠損体を創製し，「N末端アミノ基のみを標的とした部位

特異的バイオコンジュゲーション法」を確立した．このリジン欠損体に対する部位特異的バイオコンジュゲーションは，分子的均一性に優れたバイオコンジュゲート体が最大100%の収率で得られる．またリコンビナントの野生型TNF-αの場合，従来までのランダムなバイオコンジュゲーションでは僅か1分子の高分子導入により10%以下まで活性低下してしまうが，リジン欠損TNF-αに対する部位特異的バイオコンジュゲーションは殆ど活性低下を招かないなど，圧倒的な利点を有していた（図1）．この分子的均一性や比活性に優れた部位特異的PEG化リジン欠損TNF-αは，血中滞留性や抗腫瘍作用の選択的発現能にも優れているうえ，従来法で作製したランダムPEG化TNF-αよりも著しく強い*in vivo*抗腫瘍効果を有していた．一方で我々は，従来よりバイオコンジュゲート体の生体内挙動や薬効発現強度が，蛋白質表面を覆う修飾高分子の諸性質によって運命付けられることに着目し，バイオコンジュゲーション法のさらなるグレードアップを目的に，多数の機能化修飾高分子の設計を図ってきた．例えば最近，我々は腎臓への高度な薬物送達能とpH応答性薬物徐放化能を併せ持ったPVDを新規合成することに成功した（図2）．現在，上述した「プロテオーム創薬システム」によるリジン欠損機能性人工蛋白質の創製や部位特異的バイオコンジュゲーションシステムとの融合により，新たな治療戦略の確立を目指した研究を推進している．

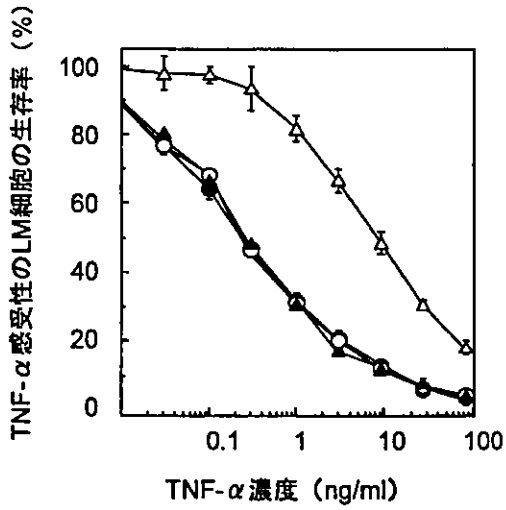

図1　リジン欠損TNF-αおよびその部位特異的バイオコンジュゲート体の*in vitro*活性評価
○，wTNF-α; △，ran-PEG-TNF-α（ランダム・モノPEG化体）; ●，リジン欠損TNF-α; ▲，sp-PEG-mTNF-α（部位特異的モノPEG化体）．

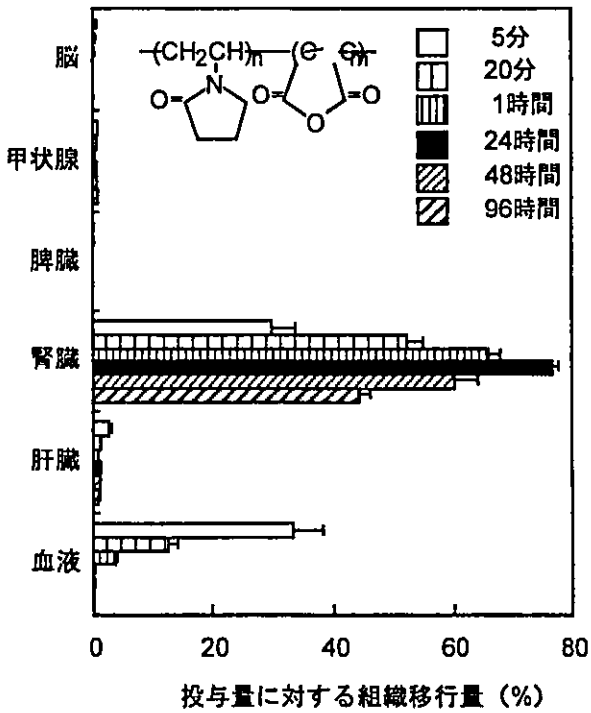

図2　PVDの静脈内投与後の組織分布

6. おわりに

以上，足早ではあるが，真弓忠範先生と共に走り続けてきた「蛋白療法の最適化に叶うDDSの開発を目指して」という道のりの極一端を紹介させて頂いた．前述したように蛋白質の臨床応用はいまだ著しく制限されており，そのほとんどは医薬品化されていない．従って，プロテオーム創薬を推進し，種々の蛋白質を有効な医薬品として適用した21世紀型蛋白療法を実現するためには，蛋白質固有の種々問題点を克服できる戦略を早急に構築せねばならない．即ち，特定レセプターへの親和性や指向性に優れたスーパーアゴニストやアンタゴニスト，体内安定性や血中滞留性に優れたミュータント等，高い安全性と有効性を保証し得る機能性人工蛋白質を，疾病や治療目的に応じて迅速かつ合理的に創出できる創薬テクノロジーの確立が不可欠である．この創薬テクノロジーは，薬剤学的観点から言えば，蛋白性薬物による疾病治療の最適化を目指したDDSであり，ポストゲノム基礎研究と21世紀医療との架け橋となり得るものと位置づけられるものと考えている．

本研究は，恩師・真弓忠範先生にご指導賜り，遂行されたものであり，また本稿の執筆に際しても格段のご配慮を賜りました．心より御礼を申し上げます．また種々ご教授頂いた共同研究者の先生方，種々ご協力頂いた大阪大学薬学研究科薬剤学分野助教授　中川晋作先生ならびに学生諸氏に深謝申し上げます．

引 用 文 献

1) Y. Yamamoto, Y. Tsutsumi, Y. Yoshioka, T. Nishibata, K. Kobayashi, T. Okamoto, Y. Mukai, T. Shimizu, S. Nakagawa, S. Nagata, T. Mayumi, Site-specific PEGylation of a lysine-deficient TNF-alpha with full bioactivity, *Nat. Biotechnol.*, **21**, 546–552 (2003).
2) Y. Kaneda, Y. Yamamoto, H. Kamada, S. Tsunoda, Y. Tsutsumi, T. Hirano, T. Mayumi, Antitumor activity of tumor necrosis factor-alpha conjugated with diviny ether and maleic anhydride copolymer on solid tumors in mice, *Cancer Res.*, **58** (2), 290–295 (1998).
3) H. Kamada, Y. Tsutsumi, Y. Yamamoto, T. Kihira, Y. Kaneda, Y. Mu, H. Kodaira, S. Tsunoda, S. Nakagawa, T. Mayumi, Antitumor activity of tumor necrosis factor-alpha conjugated with polyvinylpyrrolidone on solid tumors in mice, *Cancer Res.*, **60**, 6416–6420 (2000).
4) Y. Tsutsumi, M. Onda, S. Nagata, B. Lee, R.J. Kreitman, I. Pastan, Site-specific chemical modification with polyethylene glycol of recombinant immunotoxin anti-Tac (Fv)- PE38 (LMB-2) improves antitumor activity and reduces animal toxicity and immunogenicity, *Proc. Natl. Acad. Sci. U.S.A.*, **97**, 8548–8553 (2000).
5) H. Kamada, Y. Tsutsumi, K. Sato-Kamada, Y. Yamamoto, Y. Yoshioka, T. Okamoto, S. Nakagawa, S. Nagata, T. Mayumi, Synthesis of a poly (vinylpyrrolidone-co-dimethyl maleic anhydride) o-polymer and its application as renal targeting carrier, *Nat. Biotechnol.*, **21**, 399–404 (2003).

Available online at www.sciencedirect.com
SCIENCE DIRECT
Journal of Controlled Release 95 (2004) 229–237
journal of controlled release
www.elsevier.com/locate/jconrel

Poly(vinylpyrrolidone-co-dimethyl maleic acid) as a novel renal targeting carrier

Yoko Yamamoto [1], Yasuo Tsutsumi *,[1], Yasuo Yoshioka [1], Haruhiko Kamada, Keiko Sato-Kamada, Takayuki Okamoto, Yohei Mukai, Hiroko Shibata, Shinsaku Nakagawa, Tadanori Mayumi

Department of Biopharmaceutics, Graduate School of Pharmaceutical Sciences, Osaka University, 1-6 Yamadaoka, Suita, Osaka 565-0871, Japan

Received 18 August 2003; accepted 25 November 2003

Abstract

Poly(vinylpyrrolidone-co-dimethyl maleic acid) (PVD) was found to have high renal-targeting capability and safety as a drug carrier. To optimize the renal drug delivery system using PVD, the relationship between the molecular weight of PVD and its renal accumulation were evaluated in mice by their intravenous injection. It was found that the molecular size of 6–8 kDa was associated with the highest renal accumulation. The specific bioactivity of PVD-conjugated superoxide dismutase (SOD) relative to that of unmodified SOD gradually decreased with an increase in the degree of modification to SOD with PVD6K. The conjugated SOD (L-PVD-SOD) with the molecular size of 73 kDa, which had comparable specific bioactivity with native SOD, showed longer plasma half-life than native SOD. About sixfold more L-PVD-SOD was distributed to the kidneys than native SOD 3 h after intravenous injection, whereas extensive PVD modification did not enhance the renal accumulation of SOD. This L-PVD-SOD effectively accelerated recovery from mercuric chloride-induced acute renal failure in vivo. These results suggest that L-PVD-SOD may be the optimal derivative as a potential therapeutic agent to various renal diseases.

Keywords: Renal targeting; Vinylpyrrolidone; Dimethyl maleic acid; Polymeric carrier; Acute renal failure; Drug delivery system

1. Introduction

In recent years, clinical application of bioactive proteins, such as cytokines and growth factors, have been studied. However, most of these proteins are limited in their clinical application because of their various side effects [1,2]. In general, the plasma half-lives of bioactive proteins in vivo are very short [3–5], so that their frequent administration at a high dosage are needed to obtain sufficient therapeutic effects. This administration markedly destroys homeostasis, resulting in unexpected side effects. In addition, since bioactive proteins exhibit diverse pharmacological actions in various tissues, it is difficult to obtain only the favorable actions (therapeutic effects)

Abbreviations: DMMAn, dimethyl maleic anhydride; PVP, polyvinylpyrrolidone; VP, vinylpyrrolidone; SOD, superoxide dismutase; PVD-SOD, PVD-modified SOD; PEG, Polyethylene glycol.

* Corresponding author. Tel./fax: +81-6-6879-8178.
E-mail address: tsutsumi@phs.osaka-u.ac.jp (Y. Tsutsumi).
[1] These authors contributed equally to the work.

0168-3659/$ - see front matter © 2004 Elsevier B.V. All rights reserved.
doi:10.1016/j.jconrel.2003.11.017

selectively. To overcome their problems, bioactive proteins have been conjugated with water-soluble polymeric carriers. We have already reported that polymer conjugation of cytokines typified with tumor necrosis factor-α (TNF-α), interleukin-6 (IL-6), and immunotoxin (IT), with polyethylene glycol (PEG), and polyvinylpyrrolidone (PVP) improved its resistance to proteinase and plasma half-lives and resulted in greater therapeutic potency [6–10]. We have also shown that conjugation with polymeric carriers regulate the tissue distribution of cytokine, resulted in a selective increase its desirable therapeutic effects, and decrease its undesirable side effects. However, for further enhancement of the therapeutic potency and safety of conjugated bioactive protein, more precise control of the in vivo behavior of each protein for selective expression of their therapeutic effect is necessary. Thus, it is expected to develop novel polymeric carriers with targeting capability to specific tissue, whereas PEG and PVP are useful and powerful polymeric carriers for improving the plasma half-lives of proteins.

Renal disease is a serious problem on the increase in the world. There is no cure for renal disease, and few strategies are available for prevention [11,12]. Bioactive proteins, such as superoxide dismutase (SOD) and interleukin-10 (IL-10), have been expected to prevent the progression of renal disease, but their therapeutic potency were too low because they were poorly distributed to the kidney. The development of a renal delivery system that selectively carries drugs to the kidneys is a promising approach for limiting tissue distribution and controlling toxicity. Several renal drug delivery systems have been previously described. One approach involves prodrugs that are cleaved by kidney-associated enzymes to release the drugs in the kidney [13]. However, these prodrugs generally do not accumulate in the kidneys as a result of plasma protein binding and limited transport to the kidney. Low-molecular-weight proteins, such as lysozyme, have been used as carriers because they are reabsorbed by the kidneys. Unfortunately, they also produced strong renal toxicity and cardiovascular side effects [14]. Streptavidin carriers bind to biotin in the kidney, but they are immunogenic and have limited renal accumulation due to their large molecular size [15,16]. Thus, it is important to develop an effective renal drug delivery system that not only targets the kidney but also has excellent safety.

Recently, we synthesized poly(vinylpyrrolidone-co-dimethyl maleic acid) (PVD) as a new renal targeting carrier [17]. About 80% of the dose of PVD selectively distributed to kidneys after intravenous injection and then gradually excreted to urinary and approximately 40% remained in the kidneys 4 days after intravenous injection. No side effects occurred in the kidney and other tissues by administration of excessively high dose of PVD. In this study, to assess the usefulness of PVD as a renal targeting polymeric carrier of drugs, we first evaluated the relationship between PVD molecular weight and renal accumulation. We then prepared a conjugated SOD with PVD and evaluated the pharmacokinetic characteristics and therapeutic effects on $HgCl_2$-induced acute renal failure (ARF). This study will provide fundamental information enabling us to create a powerful drugs against renal disease.

2. Materials and methods

2.1. Synthesis and purification of PVD

Chemicals were obtained from Wako (Osaka, Japan) and 2,3-dimethyl maleic anhydride (DMMAn) was purchased from Acros Organic (New Jersey, USA). PVD was synthesized by the radical polymerization method using 4,4′-azobis-4-cyanovaleric acid (ACVA) as a radical initiator. Briefly, DMMAn and *N*-vinyl-2-pyrrolidone (VP) were mixed in a ratio of 1:5 in a glass tube containing dimethyl formamide (DMF) and incubated at 60 °C for 96 h. The resulting copolymer was precipitated in dry diethyl ether, collected immediately after filtration, and dried under vacuum. The molecular weight was determined by GFC (TSKgel G4000PW, Tosoh, Tokyo). PVD was separated into four fractions of different number-average molecular weight values. In addition, the number-average molecular weight (M_n) of each fraction was calculated by comparing it with PEG standards (Fr.1; 14 kDa, Fr.2; 8 kDa, Fr.3; 6 kDa, Fr.4; 3 kDa). The polydispersity [weight-average molecular weight (M_w)/M_n] of these PVDs were about 1.1.

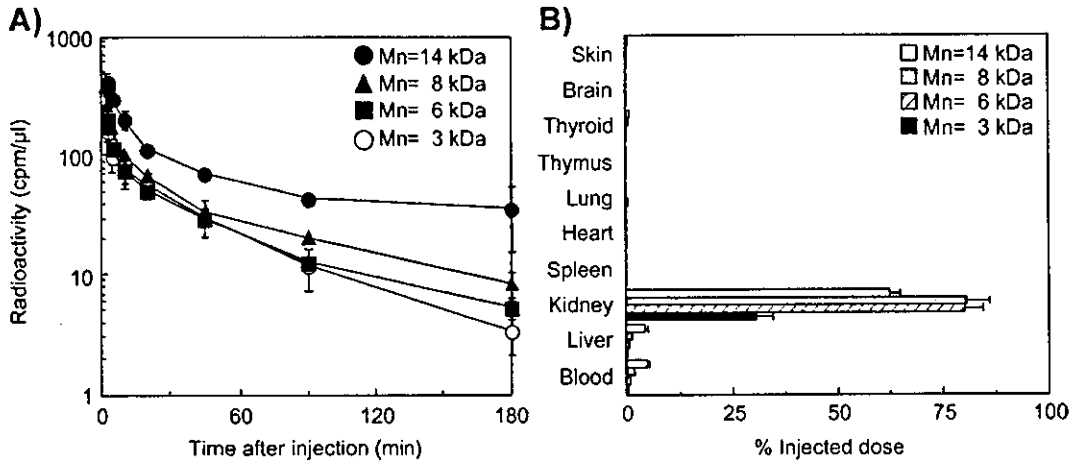

Fig. 1. Plasma clearance and tissue distribution of PVDs with various molecular weight after intravenous injection. PVD with various molecular weight were ^{125}I-labeled by chloramine-T method. Mice were intravenously injected with ^{125}I-labeled polymers. (A) After administration, blood was collected from the tail at indicated time, and the radioactivity was measured by a γ-counter. (B) At 3 h after intravenous injection, mice were sacrificed, and each organ was collected. The radioactivity was measured by a γ-counter. Data represent mean ± S.D. ($n = 5$).

2.2. Preparation of ^{125}I-labeled PVDs

To study the pharmacokinetics of PVDs with various M_n, radiolabeled PVDs were prepared by the chloramine-T method. PVDs were dissolved in DMF and activated with dicyclohexyl carbodiimide and *N*-hydroxysuccinimide for 24 h at room temperature. The PVDs were reacted with tyramine hydrochloride for 24 h at 4 °C, dialyzed in water, and lyophilized. PVD–thyramine conjugates were radiolabeled by the chloramine-T method. ^{125}I-labeled PVDs were purified by GFC. The specific activities of ^{25}I-labeled PVDs were about 4.44 μCi/mg polymer.

2.3. Measurement of plasma clearance and tissue distribution

All experimental protocols for animal studies were in accordance with the "Guide for Laboratory Animal Facilities and Care" (NIH Publication 85-23, revised 1985). These protocols have been approved by the committee in the Pharmaceutical School, Osaka University. The clearance of PVD in male BALB/c mice (5 weeks old; SLC, Hamamatsu, Japan) were studied after intravenous injection of 10 μg of polymer per mouse. Blood was collected from the tail vein at intervals, and radioactivity was measured in each sample using a γ-counter. After 3 h, most plasma ^{125}I-radioactivity was present as ^{125}I-labeled polymers and not as free ^{125}I. To evaluate tissue distribution, mice were housed in metabolic cages to collect urine and sacrificed 3 h after treatment. Clearance value was pharmacokinetically evaluated based on the clearance concept as described [18,19].

2.4. Preparation of PVD-conjugated SOD

Bovine erythrocyte Cu–Zn SOD was reacted with a 22-fold molar excess of activated PVD at room

Table 1
Clearance of PVDs with various molecular weight

Clearance (μl/h)				
	Kidney	Liver	Lung	Spleen
PVD M_n = 14 kDa	2786.4 ± 52.9	195.4 ± 13.9	10.6 ± 3.0	9.8 ± 0.4
PVD M_n = 8 kDa	6614.0 ± 199.5	119.3 ± 3.2	14.3 ± 4.4	5.7 ± 0.3
PVD M_n = 6 kDa	8888.4 ± 214.5	63.6 ± 1.4	35.2 ± 8.3	4.6 ± 0.2
PVD M_n = 3 kDa	3871.7 ± 216.8	45.4 ± 6.1	15.7 ± 7.0	3.2 ± 0.3

Mice were used in groups of five. Each value is the mean ± S.E.

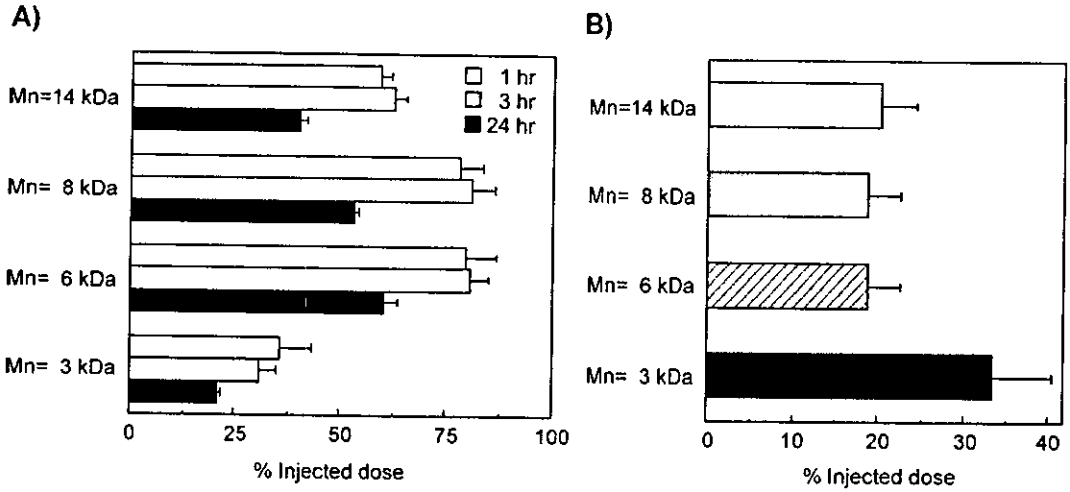

Fig. 2. Renal accumulation and urinary excretion of PVD with various molecular weight after intravenous injection. Mice were intravenously injected with ^{125}I-labeled PVDs. (A) At indicated time after intravenous injection, mice were sacrificed, and kidneys were collected. The radioactivity was counted. (B) Mice were housed in metabolic cages to collect urine for 24 h after intravenous injection. The radioactivity of urine was counted. The radioactivity was measured by a γ-counter. Data represent mean ± S.D. ($n = 5$).

temperature for 90 min in pH 8.5 borate buffer. The resultant PVD-SOD (PVD-SOD) was separated into three fraction of different molecular size (M_s) by gel filtration chromatography (Superose 12 HR10/3; Amersham Pharmacia Biotech, Uppsala, Sweden) in 0.05 M phosphate buffer (pH 7.2). The Ms of each fraction was estimated by gel filtration chromatography with protein standard (gel filtration calibration kit; Amersham Pharmacia Biotech). The specific activity of PVD-SODs was determined by the cytochrome *c* method. The biolactivity of ^{125}I-native SOD and PVD-SODs prepared by the chloramine-T method were indistinguishable from their non-radiolabeled forms.

2.5. Therapeutic effects of PVD-SOD on ARF

We used a mouse model of $HgCl_2$-induced ARF to assess the therapeutic effects of PVD-SOD (L-PVD-SOD) with M_s of 73 kDa. ARF was induced by subcutaneous injection of 8 mg/kg $HgCl_2$. Then, 12 h later, these mice were given 4 mg protein/kg native SOD or L-PVD-SOD intravenously. Therapeutic efficacy was qualitatively assessed 48 h after treatment with $HgCl_2$ by measuring the level of urinary alkaline phosphatase (ALP), urinary γ-glutamyltransferase (GTP), urinary *N*-acetyl-β-glucosaminidase (NAG), urinary glucose, urinary keton, urinary protein, urinary hemoglobin, and serum creatinine as ARF markers.

3. Results

3.1. Pharmacokinetics of PVD with various molecular weight

To evaluate the influence of molecular weight on renal accumulation of PVD, we estimated the plasma clearance and tissue distribution of PVD with various M_n after intravenous injection (Fig. 1). Radioactivity

Table 2
Characterization of PVD-conjugated SOD

	Number average[a] molecular weight	SOD enzymatic activity[b] ($\times 10^3$ U/mg)	Remaining[c] activity (%)
H-PVD-SOD	220,000	1.47 ± 0.11	63.1
M-PVD-SOD	120,000	1.97 ± 0.31	84.5
L-PVD-SOD	73,000	2.19 ± 0.05	93.9
Native SOD	32,000	2.33 ± 0.03	100.0

[a] Number-average molecular weight was determined by gel filtration HPLC (protein standard).

[b] Specific activity was measured by cytochrome *c* method. Each value represents the mean ± S.D.

[c] Remaining activity (%) was calculated base on native SOD.

[22] P.M. Tiidus, Radical species in inflammation and overtraining, Can. J. Physiol. Pharmacol. 76 (1998) 533–538.
[23] M.J. Finnen, C.M. Lawrence, S. Shuster, Inhibition of dithranol inflammation by free-radical scavengers, Lancet 2 (1984) 1129–1130.
[24] A. Guglielmotti, A. Capezzone De Joannon, N. Cazzolla, M. Marchetti, L. Soldo, G. Cavallo, M. Pinza, Radical scavenger activity of bendazac, an anticataract non-steroidal anti-inflammatory agent, Pharmacol. Res. 32 (1995) 369–373.
[25] A. Garcia-Gonzalez, J.L. Ochoa, Anti-inflammatory activity of Debaryomyces hansenii Cu, Zn-SOD, Arch. Med. Res. 30 (1999) 69–73.
[26] C. Canavese, P. Stratta, A. Vercellone, Oxygen free radicals in nephrology, Int. J. Artif. Organs 10 (1987) 379–389.
[27] T. Fujita, H. Furitsu, M. Nishikawa, Y. Takakura, H. Sezaki, M. Hashida, Therapeutic effects of superoxide dismutase derivatives modified with mono- or polysaccharides on hepatic injury induced by ischemia/reperfusion, Biochem. Biophys. Res. Commun. 189 (1992) 191–196.
[28] K. Mihara, Y. Oka, K. Sawai, Y. Takakura, M. Hashida, Improvement of therapeutic effect of human recombinant superoxide dismutase on ischemic acute renal failure in the rat via cationization anf conjugation with polyethylene glycol, J. Drug Target. 2 (1994) 317–321.

Available online at www.sciencedirect.com
SCIENCE DIRECT®
Biochemical and Biophysical Research Communications 325 (2004) 500–505
BBRC
www.elsevier.com/locate/ybbrc

Augmentation of antigen-specific immune responses using DNA-fusogenic liposome vaccine

Tomoaki Yoshikawa[a,b], Susumu Imazu[a], Jian-Qing Gao[a], Kazuyuki Hayashi[a], Yasuhiro Tsuda[a], Mariko Shimokawa[b], Toshiki Sugita[a,b], Takako Niwa[a,b], Atushi Oda[a,b], Mitsuru Akashi[b,c], Yasuo Tsutsumi[b,d], Tadanori Mayumi[e], Shinsaku Nakagawa[a,b,*]

[a] *Department of Biopharmaceutics, Graduate School of Pharmaceutical Sciences, Osaka University, Japan*
[b] *Creation of Bio-devices and Bio-systems with Chemical and Biological Molecules for Medical Use, CREST, Japan Science and Technology Corporation (JST), Japan*
[c] *Department of Molecular Chemistry, Graduate School of Engineering, Osaka University, 2-1 Yamadaoka, Suita, Osaka 565-0871, Japan*
[d] *National Institute of Health Science, Osaka Branch Fundamental Research Laboratories for Development of Medicine, 1-1-43 Hoenzaka, Chuo-ku, Osaka 540-0006, Japan*
[e] *Department of Cell Therapeutics, Graduate School of Pharmaceutical Sciences, Kobe-Gakuin University, 518 Arise, Igawadani, Nishiku, Kobe 651-2180, Japan*

Received 27 September 2004

Abstract

In an attempt to enhance the immunological efficacy of genetic immunization, we investigated a new biological means for delivering antigen gene directly to the cytoplasm via membrane fusion. In this context, we investigated fusogenic liposome (FL) encapsulating DNA as a possible genetic immunization vehicle. RT-PCR analysis indicated that a FL could introduce and express encapsulating OVA gene efficiently and rapidly in vitro. Consistent with this observation, an in vitro assay showed that FL-mediated antigen-gene delivery can induce potent presentation of antigen via the MHC class I-dependent pathway. Accordingly, immunization with FL containing the OVA-gene induced potent OVA-specific Th1 and Th2 cytokine production. Additionally, OVA-specific CTL responses and antibody production were also observed in systemic compartments including the spleen, upon immunization with the OVA-gene encapsulating FL. These findings suggest that FL is an effective genetic immunization carrier system for the stimulation of antigen-specific immune responses against its encoding antigen.

Keywords: DNA vaccine; Tumor vaccine; Liposome; Drug delivery system

Genetic immunization using plasmid DNA (pDNA) encoding antigens from bacteria, viruses, and cancers has often led to protective cell-mediated (Th1) and humoral (Th2) immunity [1]. This system has some practical advantages over conventional vaccines, such as safety, stability, cost-effectiveness for manufacturing, and the ease of modifying and customizing the gene sequence to produce the desired type of recombinant protein for expression in vivo. Although naked DNA vaccines (i.e., pDNA in saline) are effective in small animal models [2–4], recent results from large-animal and non-human primate studies have been disappointing due to sub-optimal immune responses, despite the use of multi-milligram doses of naked pDNA [5]. Therefore, the development of adjuvants and excipients to increase immune responses to DNA vaccines has become an active area of research. The potential of genetic immunization to exert an effective antigen-specific immune response is directly related to both the level of

* Corresponding author. Fax: +81 6 6879 8176.
E-mail address: nakagawa@phs.osaka-u.ac.jp (S. Nakagawa).

0006-291X/$ - see front matter © 2004 Elsevier Inc. All rights reserved.
doi:10.1016/j.bbrc.2004.10.056

expression of the encoded protein and the immunomodulatory activity generated by DNA vaccine formulations [6–8].

Two main causes for the ineffectiveness of genetic immunization have been proposed. First, the pDNAs are generally unstable in vivo. In other words, most injected pDNAs are degraded by extracellular deoxyribonucleases in situ [9–11]. In addition, a limited amount of undegraded pDNA is taken up via endocytosis by neighboring cells around the injection site, including antigen presenting cells (APCs). The endocytosed pDNAs are thus generally degraded in intracellular compartments such as endosomes or lysosomes. Consequently, extremely low levels of pDNAs that escaped from these host factors could express their encoded antigens, resulting in inefficient induction of antigen-specific immunity. Furthermore, in terms of eliciting antibody responses, DNA vaccines are poorly immunogenic relative to other vaccines such as peptide and protein vaccines [12,13]. Because of the extra- and intra-cellular degradation and low immunogenicity of naked pDNAs, genetic immunization exhibits poor performance when administered by routes other than intramuscular [5].

In this context, various approaches, such as combination with adjuvant or cytokines and particulating techniques, have been applied to enhance immune responses to the encoding antigen [9,11]. The carrier-mediated approach is particularly promising because of enhanced pDNA stability and immunogenicity, and also due to the combination with molecular adjuvants. To address these issues, several DNA-particulating approaches have been evaluated [14]. Recently, liposomes and micro- or nano-scale particles have been tested for genetic vaccination [14–20]. However, due to the low immunogenicity and degradation of pDNA by APCs, a novel carrier-mediated approach to improve the potency of DNA vaccines is required.

We previously developed a unique antigen delivery system based on liposomes fused with UV-inactivated Sendai virus, known as the fusogenic liposome, FL [21–25]. The FL efficiently delivered the encapsulated antigens into the cytoplasm of antigen presenting cells via membrane fusion for use in the MHC class I-presentation pathway [26,27]. Furthermore, FL possesses adjuvant activity derived from Sendai virus accessory proteins. It stimulates antigen presenting cells to up-regulate cell surface markers and enhances the expression of inflammatory cytokines by APCs. Additionally, we demonstrated that subcutaneous immunization with antigen-encapsulated FL induced high levels of antigen-specific immune responses at systemic immune compartments such as the spleen [26].

This information and our previous results allowed us to hypothesize that FL could be utilized as genetic vaccine carrier. Thus, the purpose of the present study was to analyze the efficiency of immunization through dermal delivery of model antigen protein-encoding DNA (OVA) delivered by FL.

Materials and methods

Mice and cells. Six- to eight-week-old male C57BL/6 (H-2^b) mice were purchased from SLC (Hamamatsu, Japan). EL4 (Tohoku University, Sendai, Japan) is a C57BL/6 T lymphoma and EG7 is an ovalbumin (OVA)-transfected clone of EL4. IC21 cells are C57BL/6 macrophage clones, H-2Kb. CD8OVA1.3 (provided by Dr. Clifford V. Harding, Case Western Reserve University, Cleveland, OH) is a T-T hybrid cell, which is specific for OVA257-264-Kb.

EL4 and IC21 cells were grown in RPMI1640 medium supplemented with 10% FCS. The CTLL-2 cells were maintained in RPMI1640 medium supplemented with 10% FCS and 1 U/ml human recombinant IL-2. The EG7 cells were maintained in RPMI1640 medium supplemented with 10% FCS and 400 μg/ml G418. CD8OVA1.3 was grown in DMEM supplemented with 10% FCS. All culture media were purchased from Invitrogen (Carlsbad, CA) and supplemented with non-essential amino acids, antibiotics and, 5×10^{-5} M 2-mercaptoethanol (2-ME).

Plasmids. The *Eco*RI fragment of pAc-neo-OVA [28] was cloned into the *Eco*RI site of pBluescriptII KS(−), resulting in pBluescriptII KS(−)/OVA. To construct an OVA gene expression vector, the *Bam*HI/*Sal*I fragment of pBluescript II KS(−)/OVA was ligated into a *Bam*HI/*Sal*I cut pCMV-script (Stratagene), resulting in pCMV-script/OVA (Fig. 1), which is driven by the cytomegalovirus promoter and contains the SV40 poly(A) signal.

Preparation of fusogenic liposome. pCMV-script/OVA containing unilamellar liposomes was prepared by a modified reverse-phase evaporation method using 46 μmol of lipids (egg phosphatidylcholine: L-α-dimyristryl phosphatidic acid: cholesterol = 5:1:4, molar ratio). After three cycles of freezing and thawing, the liposomes were sized by extrusion through a 0.8 μm polycarbonate membrane (Nucleopore; Coaster, Cambridge, USA) and pelleted by ultracentrifugation to remove unencapsulated plasmids. Then, FL encapsulated pCMV-script/OVA was prepared by fusing the liposomes with UV (2000 J/cm^2)-inactivated Sendai virus as described previously [21,26]. The amount of plasmid DNA encapsulated within liposomes was determined by means of fluorometric assay using 3,5-diaminobenzoic acid.

RT-PCR for OVA gene detection. To examine the expression of OVA mRNA, IC-21 cells were incubated in serum free RPMI1640

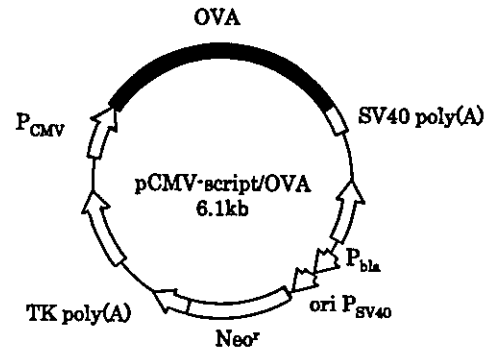

Fig. 1. Structure of OVA expression plasmid pCMV-script/OVA. OVA cDNA was inserted into an expression plasmid (pCMV-script) containing a cytomegalovirus (CMV) promoter and a SV40 polyadenylation site.

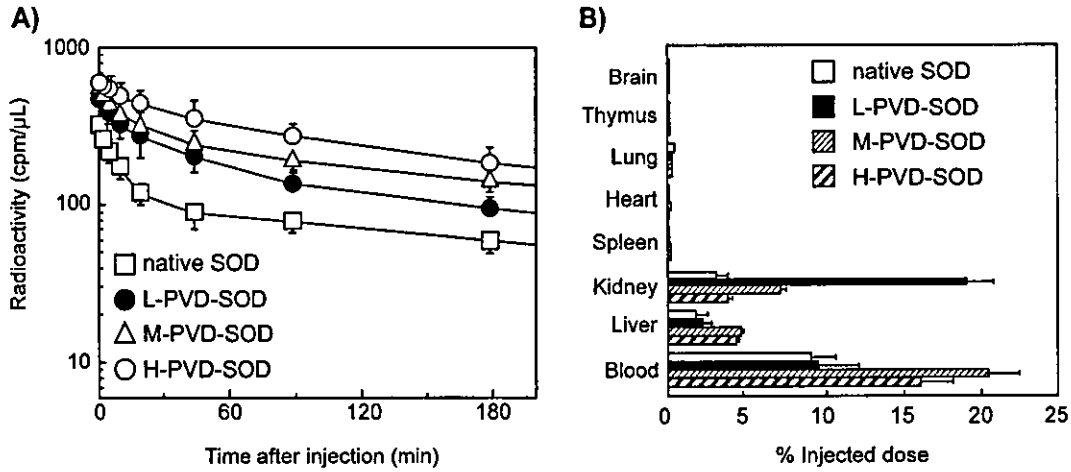

Fig. 3. Plasma clearance and tissue distribution of native SOD and PVD-SODs 3 h after intravenous injection. Mice were intravenously injected with ^{125}I-labeled native SOD and PVD-SODs. (A) After administration, blood was collected from the tail at indicated time, and the radioactivity was counted. (B) Each organ was removed 3 h after intravenous injection, and radioactivity was counted. Data was represented at % injected dose. The radioactivity was measured by a γ-counter. Data represent mean ± S.D. ($n = 5$).

in the supernatant of homogenized kidneys was measured after acid precipitation to distinguish between bound polymer and free tyramine, it has been confirmed that the PVD did not release the free tyramine and it was not degraded in the kidneys (data not shown). The blood retention increased as the molecular weight increased (Fig. 1A). On the other hand, PVD with an average molecular weight of 6–8 kDa [PVD_{6k} and PVD_{8k}] showed highest renal accumulation and about 80% of the administered dose accumulate in the kidneys at 3 h after injection (Fig. 1B). Accumulation rates decreased to 60% for PVD_{14k} and to 30% for PVD_{3k}. Table 1 summarizes the clearance calculated based on the radioactivity at 3 h after intravenous injection of various PVDs in mice. The uptake clearance of PVD_{6k} were the highest among various PVDs. Similar trends in results were noted at 1 and 24 h (Fig. 2A). PVD_{6k} and PVD_{8k} were rapidly eliminated from blood and specifically accumulated in the kidneys only 1 h after intravenous injection without distribution to other tissues. In addition, PVD_{6k} and PVD_{8k} showed high retention in the kidneys and about 60% of injected dose retained in the kidneys 24 h after intravenous administration. By the measurement of the urinary radioactivity excretion, it became clear that the PVD which accumulated in the kidney was gradually excreted urinary. Furthermore, measurement of urinary radioactivity excretion revealed a significantly higher value for PVD_{3k} with the lowest M_n (Fig. 2B).

3.2. Characteristics of PVD-SOD

The PVD-SOD was prepared via formation of amide bond between SOD lysine residues and carboxyl groups of PVD_{6k}. The resultant PVD-SOD was separated into three fraction of different molecular size (high = H, middle = M, low = L) by gel filtration HPLC, and then, specific activities were measured. The separated PVD-SODs, with molecular size of 73, 120, and 220 kDa, were termed L-PVD-SOD, M-PVD-SOD, H-PVD-SOD, respectively. Table 2 shows characterization of PVD-SODs. Although specific activity decreased with increasing molecular size, even H-PVD-SOD with the largest molecular size still had 60% activity compared with native SOD.

Table 3
Clearance of native SOD and PVD-SODs

Clearance (μl/h)				
	Kidney	Liver	Lung	Spleen
H-PVD-SOD	18.0 ± 0.3	20.1 ± 0.5	1.7 ± 0.2	1.1 ± 0.1
M-PVD-SOD	31.9 ± 1.2	20.9 ± 0.2	2.0 ± 0.1	1.1 ± 0.1
L-PVD-SOD	182.6 ± 9.3	20.3 ± 2.3	3.6 ± 0.3	1.4 ± 0.1
Native SOD	34.1 ± 4.9	19.9 ± 3.0	5.3 ± 0.9	1.4 ± 0.2

Mice were used in groups of five. Each value is the mean ± S.E.

Table 4
Therapeutic effects of L-PVD-SOD to $HgCl_2$-induced ARF

		Intact mice	ARF mice	Native SOD-treated ARF mice	L-PVD-SOD-treated ARF mice
Urinary levels	hemoglobin	− (<0.06 mg/dl)	++ (>0.75 mg/dl)	+	−
	ketone	− (<5 mg/dl)	++ (>20 mg/dl)	±	−
	glucose	− (<100 mg/dl)	++ (>2000 mg/dl)	+	±
	protein	− (<10 mg/dl)	++ (>1000 mg/dl)	+	±
	γ-GTP	− (<0.7 IU/LOG)	++ (>550 IU/L)	++	+
	ALP	− (<14 IU/l)	++ (>400 IU/l)	+	±
	NAG	− (<12 IU/l)	++ (>17 IU/l)	++	−
Serum levels	creatinine	− (<0.5 mg/dl)	++ (>1.5 mg/dl)	+	±

We used a mouse model of $HgCl_2$-induced ARF to assess the therapeutic effects of L-PVD-SOD. ARF was induced by subcutaneous injection of 8 mg/kg $HgCl_2$, and then, these mice were given 4 mg protein/kg native SOD or L-PVD-SOD intravenously. Therapeutic efficacy was qualitatively assessed 48 h after treatment with $HgCl_2$ by measuring the level of urinary alkaline phosphatase (ALP), urinary γ-glutamyl transferase (GTP), urinary *N*-acetyl-β-glucosaminidase (NAG), urinary glucose, urinary keton, urinary protein, urinary hemoglobin, and serum creatinine as ARF markers. Mice were used in groups of five. −: negative; ±: quasi-positive; +: weak positive; ++: strong positive.

3.3. Pharmacokinetics of PVD-SOD

We then evaluated pharmacokinetics of three kinds of PVD-SODs after intravenous administration. Native SOD was rapidly cleared from the blood circulation (Fig. 3A). Three hours after injection, little accumulation of native SOD into the kidneys was observed (Fig. 3B), and almost all native SOD was found to be eliminated in the urine (data not shown). On the other hand, the blood residency and renal distribution of PVD-SOD increased with decreasing their molecular size. For L-PVD-SOD with almost full activity compared with native SOD, its renal accumulation was about six times higher than that of native SOD, and L-PVD-SOD did not show with selective distribution to other major organs such as the liver or spleen. M-PVD-SOD and H-PVD-SOD showed higher distribution to liver than native SOD and L-PVD-SOD, probably due to their high blood concentration. Table 3 summarizes the clearance calculated based on the radioactivity at 3 h after intravenous injection of native SOD and three kinds of PVD-SODs in mice. This data also showed that L-PVD-SOD accumulated in kidney specifically.

3.4. Therapeutic effect of L-PVD-SOD on ARF

We also assessed the therapeutic effect of L-PVD-SOD on ARF (Table 4). ARF was induced by subcutaneous injection of $HgCl_2$ at a dose of 8 mg/kg. Not only the levels of urinary ALP, γ-GTP, NAG, and serum creatinine, but also the urinary content of hemoglobin, keton, glucose, and protein rapidly increased 12 h later. Native SOD and L-PVD-SOD at a dose of 4 mg protein/kg were injected intravenously 12 h after injection of $HgCl_2$. The therapeutic efficacy were assessed 48 h after administration of $HgCl_2$ (Table 4), because ARF markers reached the highest levels in untreated ARF mice. Native SOD showed weak therapeutic effects, but L-PVD-SOD effectively accelerated recovery from ARF.

4. Discussion

The in vivo pharmacokinetics of polymer-conjugated drugs, such as bioactive proteins, may be markedly influenced by the properties of the polymeric carriers, such as electric charge and hydrophilic/hydrophobic balances, attached to the surface of the drugs. Therefore, to achieve optimization of drug therapy by polymer conjugation typified by PEGylation, we must initially design polymeric carrier with useful functions such as targeting and controlled release capability, which can regulate closely their behavioral characteristics in vivo. We previously reported that polyvinylpyrrolidone (PVP) was more suitable polymeric carrier for enhancing the blood residency of drugs than PEG [8]. Using this PVP as a backbone polymer, we have evaluated

the in vivo pharmacokinetics of synthesized PVP derivatives with various electrically charge or hydrophilic/hydrophobic balance [20]. For instance, the co-polymer between vinylpyrrolidone (VP) and vinyl-lauric acid showed a marked increase in distribution in the spleen compared to that in the liver. Recently, we synthesized a novel polymeric drug carrier, PVD, which was a powerful candidate as a targeting carrier for a renal drug delivery system. In this study, we attempted to optimize the renal drug delivery system using PVD.

To assess the usefulness of PVD as a renal targeting carrier, the relationship between the M_n of PVD and its renal accumulation after intravenous injection was investigated (Fig. 1). Renal accumulation was highest for molecules with an M_n of 6–8 kDa, about 80% of the administered dose accumulate in the kidneys 3 h after intravenous injection. Increase or decrease of an M_n lowered the renal accumulation (Fig. 2). We have previously showed that the safety of PVD was similar to that of PEG and PVP, which are used clinically [17]. Thus, PVD with 6–8 kDa of M_n seems to be an extremely safe polymeric carrier with much higher renal targeting and retention capacity. It has previously been found that PVD was selectively accumulated in renal proximal tubular epithelial cells after intravenous injection [17]. Additionally, the uptake of PVD by renal tubular cells was inhibited by the energy inhibitor (NaN_3) and was not affected by cytochalasin B. Thus, PVD may be taken in by an energy-dependent process except for endocytosis. Several specific molecules play a role in renal transport, and various organic anions transporter exist in the kidney, but these transporters generally carry low-molecular-weight drugs. It is unclear why PVD with a molecular weight of 6–8 kDa was selectively accumulated in the kidneys. To address this question, we are currently in the process of doing some experiments.

We further evaluated the usefulness of PVD as a renal targeting carrier by polymer conjugation to SOD, which has been expected to be a potential drug to renal disease. Many recent studies have reported an association between activated oxygen species such as superoxide radical (O_2^-), hydrogen peroxide (H_2O_2), hydroxyl radical (·OH), and NO with various pathologic disease processes such as cancer, inflammation, septicemia, and necrosis associated with ischemic reperfusion [21,22]. Several studies have investigated the use of activated oxygen metabolic enzymes and antioxidants as therapeutic agents in diseases where stress oxidation plays a prominent role [23,24]. SOD has shown promise as a therapeutic agent, eliminating O_2^- in the early stages of formation of highly reactive oxygen species such as ·OH. Developments in genetic engineering have now enabled the production of large quantities of human Cu/Zn-SOD, which has attracted attention as a therapeutic agent [25]. With respect to kidney disease, activated oxygen is known to play an indispensable role in the mechanisms of ARF, complications associated with long-term maintenance dialysis, drug toxicity, and various inflammatory conditions [26]. We prepared PVD-SODs with various molecular size (Table 2) and then evaluated their tissue distribution 3 h after intravenous injection (Fig. 3). The renal accumulation of PVD-SODs decreased with increasing their molecular size. About sixfold more L-PVD-SOD with 73 kDa of M_n, which had almost full activity compared with native SOD, was distributed to the kidneys than native SOD. The renal accumulation of PVP-modified SOD with the same molecular size as L-PVD-SOD was similar to that of native SOD (data not shown). This confirms that renal accumulation of L-PVD-SOD is attributable to the properties of PVD. However, extensive PVD modification of SOD did not increase its renal accumulation. These results indicated that L-PVD-SOD was the optimal derivative which had a potential renal targeting capability. Thus, our results revealed that the renal accumulation probably involves not only an optimal introduction rate of electrical charges and/or hydrophobicity to PVD, but also molecular size of PVD-SOD.

Renal disease is one of the most serious problems in the world. Many researchers have attempted to deliver drug to the kidney. For example, Hashida et al. reported that cationized SOD and PEGylated SOD exhibited significant therapeutic effects on ischemic acute renal failure [27,28]. However, there is no report as to delivery of drug to the kidney specifically. On the other hand, PVD accumulated in the kidney about 80% of the administered dose. Therefore, we consider that PVD may be the most superior carrier for delivering drug to the kidney. Thus, the development

of new therapeutic approaches is expected for treating patients with renal disease. As shown in Table 4, L-PVD-SOD showed great potential as a renal antioxidant agent to ARF. These results suggest that L-PVD-SOD may be a candidate as a novel therapeutic agent with high renal targeting capability.

Acknowledgements

This study was supported in part by a Grant-in-Aid for Scientific Research (No. 15680014) from the Ministry of Education, Science and Culture of Japan, in part by Health Sciences Research Grants for Research on Health Sciences focusing on Drug Innovation from the Japan Health Sciences Foundation (KH63124), and in part by Takeda Science Foundation.

References

[1] M. Blick, S.A. Sherwin, M. Rosenblum, J. Gutterman, Phase I study of recombinant tumor necrosis factor in cancer patients, Cancer Res. 47 (1987) 2986–2989.

[2] S.A. Rosenberg, M.T. Lotze, L.M. Muul, A.E. Chang, F.P. Avis, S. Leitman, W.M. Linehan, C.N. Robertson, R.E. Lee, J.T. Rubin, et al., A progress report on the treatment of 157 patients with advanced cancer using lymphokine-activated killer cells and interleukin-2 or high-dose interleukin-2 alone, N. Engl. J. Med. 316 (1987) 889–897.

[3] J.H. Donohue, S.A. Rosenberg, The fate of interleukin-2 after in vivo administration, J. Immunol. 130 (1983) 2203–2208.

[4] A.P. Bollon, S.L. Berent, R.M. Torczynski, N.O. Hill, Y. Lemeshev, J.M. Hill, F.L. Jia, A. Joher, S. Pichyangkul, A. Khan, Human cytokines, tumor necrosis factor, and interferons: gene cloning, animal studies, and clinical trials, J. Cell. Biochem. 36 (1988) 353–367.

[5] H. Tanaka, T. Tokiwa, Influence of renal and hepatic failure on the pharmacokinetics of recombinant human granulocyte colony-stimulating factor (KRN8601) in the rat, Cancer Res. 50 (1990) 6615–6619.

[6] Y. Tsutsumi, M. Onda, S. Nagata, B. Lee, R.J. Kreitman, I. Pastan, Site-specific chemical modification with polyethylene glycol of recombinant immunotoxin anti-Tac(Fv)-PE38 (LMB-2) improves antitumor activity and reduces animal toxicity and immunogenicity, Proc. Natl. Acad. Sci. U. S. A. 97 (2000) 8548–8553.

[7] Y. Kaneda, Y. Yamamoto, H. Kamada, S. Tsunoda, Y. Tsutsumi, T. Hirano, T. Mayumi, Antitumor activity of tumor necrosis factor-alpha conjugated with divinyl ether and maleic anhydride copolymer on solid tumors in mice, Cancer Res. 58 (1998) 290–295.

[8] H. Kamada, Y. Tsutsumi, Y. Yamamoto, T. Kihira, Y. Kaneda, Y. Mu, H. Kodaira, S. Tsunoda, S. Nakagawa, T. Mayumi, Antitumor activity of tumor necrosis factor-alpha conjugated with polyvinylpyrrolidone on solid tumors in mice, Cancer Res. 60 (2000) 6416–6420.

[9] Y. Yamamoto, Y. Tsutsumi, Y. Yoshioka, T. Nishibata, K. Kobayashi, T. Okamoto, Y. Mukai, T. Shimizu, S. Nakagawa, S. Nagata, T. Mayumi, Site-specific PEGylation of a lysine-deficient TNF-alpha with full bioactivity, Nat. Biotechnol. 21 (2003) 546–552.

[10] Y. Tsutsumi, S. Tsunoda, H. Kamada, T. Kihira, Y. Kaneda, Y. Ohsugi, T. Mayumi, PEGylation of interleukin-6 effectively increases its thrombopoietic potency, Thromb. Haemost. 77 (1997) 168–173.

[11] C.A. Jones, G.M. McQuillan, J.W. Kusek, M.S. Eberhardt, W.H. Herman, J. Coresh, M. Salive, C.P. Jones, L.Y. Agodoa, Serum creatinine levels in the US population: third National Health and Nutrition Examination Survey, Am. J. Kidney Dis. 32 (1998) 992–999.

[12] F.N. Ziyadeh, S. Goldfarb, The diabetic renal tubulointerstitium, Curr. Top. Pathol. 88 (1995) 175–201.

[13] A.A. Elfarra, et al., Targeting 6-thioguanine to the kidney with *S*-(guanin-6-yl)-L-cysteine, J. Pharmacol. Exp. Ther. 274 (1995) 1298–1304.

[14] R.F. Haverdings, et al., Potentials and limitations of the low-molecular-weight protein lysozyme as a carrier for renal drug targeting, Renal Failure 23 (2001) 397–409.

[15] B. Schechter, R. Arnon, C. Colas, T. Burakova, M. Wilchek, Renal accumulation of streptavidin: potential use for targeted therapy to the kidney, Kidney Int. 47 (1995) 1327–1335.

[16] R.J. Kok, F. Grijpstra, R.B. Walthuis, F. Moolenaar, D. de Zeeuw, D.K. Meijer, Specific delivery of captopril to the kidney with the prodrug captopril-lysozyme, J. Pharmacol. Exp. Ther. 288 (1999) 281–285.

[17] H. Kamada, Y. Tsutsumi, K. Sato-Kamada, Y. Yamamoto, Y. Yoshioka, T. Okamoto, S. Nakagawa, S. Nagata, T. Mayumi, Synthesis of a poly(vinylpyrrolidone-co-dimethyl maleic anhydride) co-polymer and its application as renal targeting carrier, Nat. Biotechnol. 21 (2003) 399–404.

[18] M. Nishikawa, Y. Takakura, M. Hashida, Pharmacokinetic evaluation of polymeric carriers, Adv. Drug Deliv. Rev. 21 (1996) 135–155.

[19] M. Nishikawa, T. Nakano, T. Okabe, N. Hamaguchi, Y. Yamasaki, Y. Takakura, F. Yamashita, M. Hashida, Residualizing indium-111-radiolabel for plasmid DNA and its application to tissue distribution study, Bioconjug. Chem. 14 (2003) 955–961.

[20] H. Kodaira, Y. Kaneda, Y. Yamamoto, T. Namba, Y. Tsutsumi, T. Hirano, T. Mayumi, Fundamental study on molecular design of bioconjugated drugs with water-soluble polymeric modifiers; influence of electric charge on pharmacokinetics of water-soluble polymers, Drug Deliv. Syst. 12 (1997) 431–437.

[21] A. Hamvas, R. Palazzo, L. Kaiser, J. Cooper, T. Shuman, M. Velazquez, B. Freeman, D.P. Schuster, Inflammation and oxygen free radical formation during pulmonary ischemia-reperfusion injury, J. Appl. Physiol. 72 (1992) 621–628.

medium for 10 min at 37 °C with FL containing pCMV-script/OVA (1 μg), Lipofectin (Invitrogen) complexed with 1 μg plasmid as described in the manufacturer's protocol. After 24 h cultivation, total RNA was extracted from the transfected cells and used as a template for RT-PCR analysis.

Antigen presentation assay. The in vitro assay for antigen processing and presentation was performed as described in other studies [26]. In brief, IC21 cells (10^5 cells/well in 96-well plate) were incubated with various concentrations of antigens-encoding plasmids entrapped or complexes with various vectors at 37 °C for only 10 min. The cells were washed and subsequently incubated at 37 °C for 24 h. Then the cells were fixed with 0.05% glutaraldehyde, washed three times, and cultured with CD8OVA1.3 T hybridoma cells (10^5 cells/well). The response of the CD8OVA1.3 T cells was determined by the level of IL-2 secretion using a CTLL-2 proliferation assay. Results are expressed as means ± SD for triplicate/group.

Detection of OVA-specific antibody production by ELISA. OVA-specific antibody was detected as described previously. ELISA plates were coated with 10 mg/ml OVA in 50 mM bicarbonate buffer. Wells were blocked with 2-fold diluted Block Ace (Dai-Nippon Pharmaceutical) for 16 h at 4 °C. After washing four times with PBS containing 0.05% Tween 20 (PBS-T), each diluted serum was added (50 μl/well) and incubated for 2 h at 37 °C. Serums from non-immunized mice were included as controls. HRP conjugated anti-mouse IgG1 (Southern Biotechnology Associates, Birmingham, AL) was used as the detection Ab. Following 2 h incubation at 37 °C, plates were washed, and the reaction was developed by 3,3′,5,5′-tetramethylbenzidine (Moss, Pasadena, CA), and color development was terminated after a 15-min incubation by addition of 2 N H_2SO_4. Endpoint titers were expressed as the reciprocal log2 of the last dilution, which gave an OD at 450 nm of 0.1 greater than non-immunized mice.

Cytokine analysis by ELISA. Cytokine levels in culture supernatants of Ag-stimulated splenocytes were determined by a cytokine-specific ELISA. Briefly, splenocytes from immunized mice were cultured with 1 mg/ml OVA. Culture supernatants were harvested 96 h after incubation, and the levels of Th1 (IFN-γ) and Th2 (IL-4, IL-5, and IL-6)-type cytokines were determined by cytokine-specific ELISA kit (Amersham–Pharmacia Biotech). The concentration of cytokines was calculated by standard curves obtained according to the instruction provided by the manufacturer.

In vitro CTL induction and cytotoxic assay. C57BL/6 mice (7 weeks old, male, H-2b) were immunized twice at two-week intervals with 50 μg of naked DNA, cationic lipid/plasmid complex, and plasmids entrapped in a conventional liposome or FL. Spleen cells from immunized or non-immunized mice were recovered 14 days after the last immunization and were stimulated in vitro with mitomycin C-treated EG7 cells for 5 days. The cytotoxic activity of these effector cells was tested on ^{51}Cr-labeled target cells, OVA-expressed EG7 cells, and EL4 as a control, at various effector/target ratios. The cytotoxicity assay was completed in triplicate. The maximum release was determined by adding 1% Triton X-100 to the target cells. A spontaneous release was obtained in target cells incubated without effector cells. EL4 cells were used as control for specificity. The released radioactivity was measured in the supernatant. The specific lysis was determined as follows: percentage of specific lysis = [(percentage of lysis of positive target) − (percentage of lysis of negative target)].

Tumor rejection assay. C57BL/6 mice were immunized twice s.c. at the tail base using three doses of naked DNA, cationic lipid/plasmid complex, and plasmids entrapped in a conventional liposome or a FL at two-week intervals. Fourteen days after the last immunization (day 0), 1×10^6 OVA-expressing EG7 cells or 1×10^6 EL4 cells were intradermally injected. Six to thirteen mice were used for each experimental group. Tumor growth was monitored by calculating the tumor volume and was individually plotted. The tumor volume was calculated as follows: $V = (\text{length} \times \text{width}^2)/2$. Tumor measurements were determined until they exceeded 1000 mm^3.

Results and discussion

Initially, using RT-PCR analysis, we verified the expression of OVA mRNA transcribed from the plasmid, pCMV-script/OVA (Fig. 1), used for DNA vaccination (Fig. 2, lane a). We also performed in vitro transfection studies to assess the OVA proteins expressed in a transfected mouse macrophage cell line (IC-21) and fibroblasts (L cells). It appears that a majority of the DNA injected in vivo is rapidly degraded by extracellular deoxyribonucleases. In this regards to intimate the in vivo milieu, in vitro transfection experiments were performed for only 10 min. Surprisingly, in only 10 min transfection, a remarkably higher OVA mRNA expression was detected in IC-21 and L cells treated with FL than by other transfection techniques (Fig. 2, naked plasmid, lane b; liposome, lane c; Lipofectin, lane d; and FL, lane e). For example, OVA expression was lower for a commercially available cationic lipid-based gene delivery method (Lipofectin) than for FL-mediated transfection in L cells. Furthermore, OVA expression was not observed in IC-21 cells in response to the Lipofectin method.

We have demonstrated that FLs deliver their contents via membrane fusion rather than endocytosis and that macrophages preferentially phagocytize positively charged liposomes [29,30]. Together, these studies indicate that plasmid vectors complexed with cationic lipids are taken up through an endocytotic pathway and degraded in endosomes. In contrast, FLs mediate rapid and efficient introduction of the encapsulated plasmid into cells, which leads to antigen processing and presen-

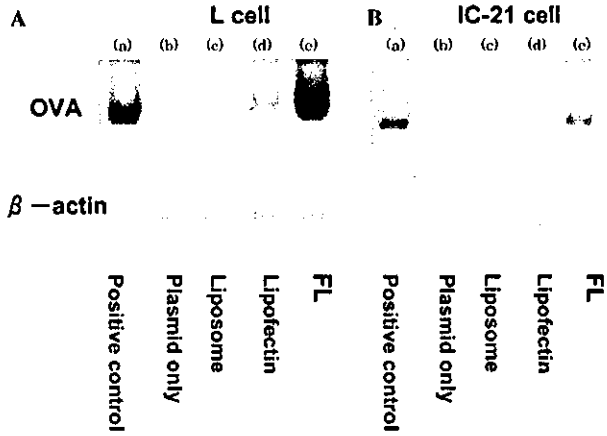

Fig. 2. RT-PCR analysis of OVA in L and IC-21 cells that were transfected by various vectors. L (A) and IC-21 (B) cells were incubated with various vectors at 37 °C for 10 min. after 24 h in culture. Naked 1 μg pCMV-script/OVA plasmid (b), conventional liposome encapsulating 1 μg pCMV-script/OVA (c), 5 μg Lipofectin/pCMV-script/OVA complex (d), and 1 μg pCMV-script/OVA-FL (e) were co-amplified by *Taq* DNA polymerase generating 864 bp PCR fragments. The samples were electrophoresed through a 2.0% agarose gel and stained with ethidium bromide.

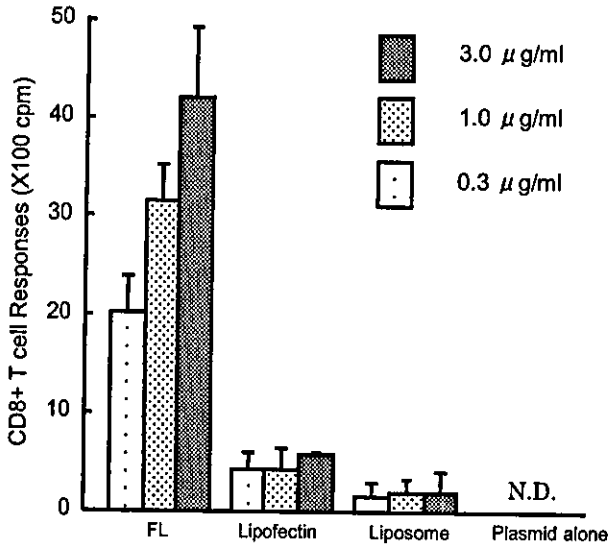

Fig. 3. Presentation of OVA using FL on MHC class I molecules by IC-21 cells. IC-21 cells were incubated with various concentrations of antigen-encoding plasmids entrapped or complexed with various vectors at 37 °C for only 10 min. After 24 h in culture, the IC-21 cells were incubated with CD8OVA1.3 T hybridoma cells for 24 h. The responses of CD8OVA1.3 were determined by their level of IL-2 secretion, using a CTL bioassay. Results are expressed as means ± SD for each group ($n = 3$).

tation to MHC class I molecules in a murine macrophage cell line (IC-21) (Fig. 3).

In the present study, we also investigated anti-OVA IgG responses in mice after subcutaneous immunization with FL. We collected blood samples from mice at the indicated time points after immunization with pCMV-script/OVA-FL and several other plasmid formulations. Both IgG1 and IgG2a antibodies were assessed by ELISA against recombinant OVA proteins (Fig. 4). The OVA-specific IgG1 and IgG2a responses in the serum of mice subcutaneously immunized with pCMV-script/OVA-FLs were remarkably higher than those from mice immunized with naked plasmid, pCMV-script/OVA encapsulated conventional liposome, or Lipofectin/pCMV-script/OVA complexes. These serum Ab responses remained elevated for at least 12 weeks and demonstrated that FL-mediated antigen expression induced efficient and antigen-specific humoral immune responses.

In general, DNA vaccines that do not use an immuno-modulating adjuvant (CpG oligonucleotides, cholera-toxin, and heat-labile toxin) exhibit low immunogenicity [6,13,16,17]. These observations are supported by the results of human trials of DNA vaccination, which are generally ineffective [1]. In this regard, the development of a delivery system for DNA vaccination, which possesses immuno-potentiating adjuvant activity, is desirable. We therefore characterized the Ag-specific splenocytes from mice subcutaneously immunized with pCMV-script/OVA-FLs, and determined Th1 (IFN-γ) and Th2 (IL-4)-specific cytokine production levels (Table 1). Th1- and Th2-type cytokine production in splenocytes increased remarkably in mice immunized with pCMV-script/OVA-FLs. These results indicated that FLs could elicit systemic Th1- and Th2-type CD4+ T cells without co-administration of adjuvants.

As indicated in Fig. 4, Th1-type Ag-specific responses were also induced by FL-mediated DNA vaccination, which suggests that this method could induce efficient and Ag-specific CTL responses. To confirm this theory we performed an in vitro cytotoxicity assay. CTL activity of splenocytes from mice immunized with pCMV-script/OVA-FLs against EG7 cells was stronger than that of splenocytes from mice immunized with other pDNA formulations, such as naked pDNA, Lipofec-

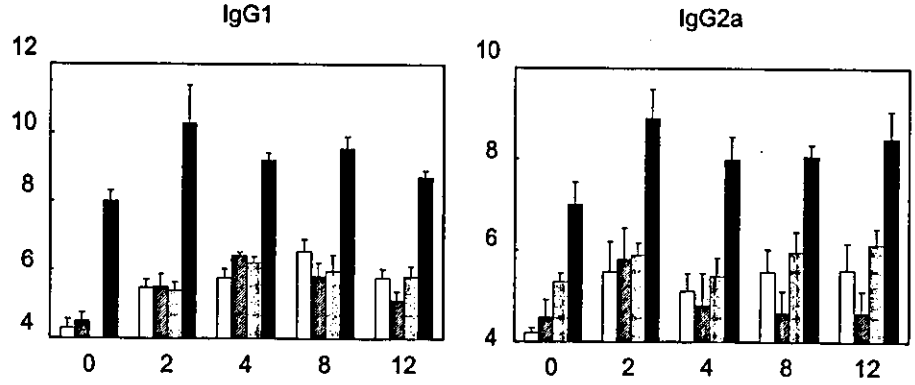

Fig. 4. OVA-specific Ab responses after intradermal immunization with pCMV-script/OVA-FL. Balb/c mice were immunized with 50 μg of naked pCMV-script/OVA (□), 5 μg conventional liposome encapsulating pCMV-script/OVA (▨), 25 μg of a Lipofectin/5 μg pCMV-script/OVA complex (▩), or 5 μg pCMV-script/OVA-FL (■) twice with an interval of two weeks between treatments. Serum samples were collected from each mouse and assayed for OVA-specific IgG1 and IgG2a by ELISA at different time intervals after the primary immunization. Titers were defined as the highest dilution required to reach an OD of 0.1 at 450 nm.

Table 1
Characterization of Th1- and Th2-responses in vivo

Vector	Stimulation	IFN-γ (pg/ml)	IL-4 (pg/ml)
Saline	Medium	157.0 ± 12.7	<7.8
	OVA	161.4 ± 15.3	<7.8
Naked DNA	Medium	170.4 ± 26.4	10.3 ± 2.5
	OVA	443.8 ± 39.5	11.5 ± 1.8
Liposome	Medium	165.7 ± 10.7	9.5 ± 1.5
	OVA	438.1 ± 21.4	9.8 ± 1.2
Cationic liposome	Medium	182.6 ± 14.6	12.8 ± 1.7
	OVA	529.4 ± 25.7	11.4 ± 2.4
Fusogenic liposome	Medium	176.1 ± 18.4	12.4 ± 2.4
	OVA	861.1 ± 58.4	24.2 ± 3.7

Splenocytes (5×10^6 cells/ml) were stimulated in vitro for 48 h with OVA protein (1 mg/ml), and the cytokine levels in the culture supernatant were determined by ELISA. The mean ± SD is shown for each group of three mice. The lower limit of IL-4 detection was 7.8 pg/ml.

tin/pDNA complexes or pDNA encapsulated by conventional liposomes. These findings emphasize that plasmid DNA vaccination combined with FL could induce effective CTL responses (Fig. 5).

Finally, we investigated whether FL-mediated DNA vaccination could induce antigen-specific anti-tumor immunity. In order to determine the effects of FL-mediated prophylactic vaccination, we analyzed tumor growth and survival after vaccination in the EG7 model.

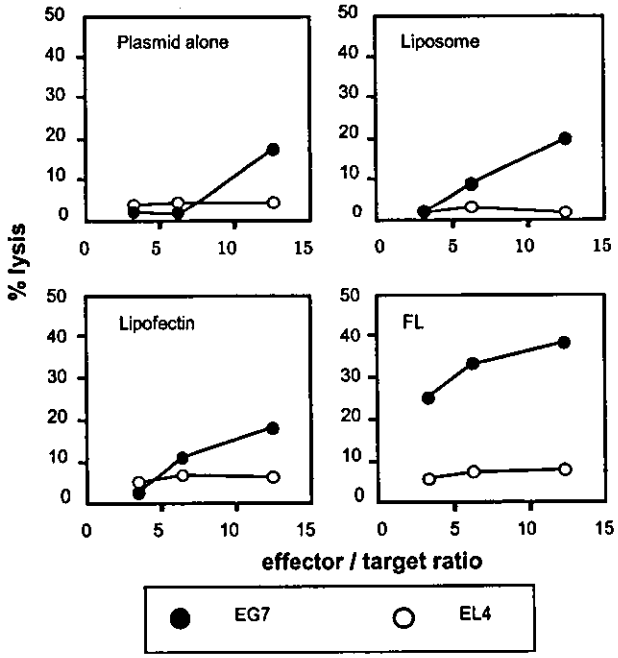

Fig. 5. In vivo immunization with pCMV-script/OVA encapsulated by FL induced antigen-specific CTL responses. Fourteen days after the last immunization, splenocytes from mice immunized with naked pCMV-script/OVA (50 μg), pCMV-script/OVA (5 μg) encapsulated by a conventional liposome, Lipofectin/pCMV-script/OVA (25 μg) complex or FL containing pCMV-script/OVA (5 μg) were isolated and restimulated with MMC-treated EG7 for 5 days to enhance the frequency of Ag-specific CTLs. CTL activity against EG7 or EL4 was measured by a ^{51}Cr release assay. The figure represents the amount of lysis against the ^{51}Cr-labeled EG7 and EL4.

Four weeks after the last immunization, mice were intradermally challenged with 10^6 live EG7 cells in the abdomen. As shown in Fig. 6, high concentrations of naked pCMV-script/OVA, 5 μg pCMV-script/OVA/Lipofectin complexes or pCMV-script/OVA encapsulated in conventional liposomes did not generate protective immunity. In contrast, only 5 μg of pCMV-script/OVA encapsulated in FL exhibited enhanced anti-tumor effects as demonstrated by reduced tumor growth and prolonged survival. Furthermore, Hayashi and Kunisawa et al. reported that FL possesses immuno-stimulating activities derived from Sendai virus accessory proteins displayed on the FL surface, which up-regulate co-stimulatory molecules on cells, including antigen presenting cells such as dendritic cells and splenocytes [27,31]. In the present study, in vitro experiments provide evidence that FLs mediate efficient introduction and expression of antigen genes and enhance MHC class I antigen presentation. Our findings lead us to surmise that these synergistic effects facilitated antigen-specific immune reactions in response to FLs used as genetic vaccine carriers.

Our results demonstrated that FL-mediated genetic immunization can trigger strong and antigen-specific humoral and cell-mediated immunity in mice. FL, which was reconstituted from UV-inactivated Sendai virus and liposomes, is a promising approach for antigen-encoding gene delivery. Sendai virus-derived accessory proteins incorporated into FL not only enhance antigen introduction into the cytoplasm and pDNA expression, but also stimulate inflammatory responses, a major advantage of DNA vaccination. In conclusion, our present study illustrated that FL-mediated genetic vaccination facilitates the antigen presentation by APC in vitro and remarkably enhanced anti-tumor immune responses in vivo. Thus, by overcoming the current problems in genetic immunization, the FL-mediated gene transfer system makes significant progress toward the development of genetic cancer or viral vaccines.